Snake-like Motion Controller Design with TMS320C6713 DSP Processor

R. P. CHATTERJEE [*1], UMA DUTTA[*]
*Scientist, Central Mechanical Engineering Research Institute,
M.G. Avenue, Durgapur-713209
INDIA
1 Member, IEEE Communication Society
r_chatterjee@cmeri.res.in, umadutta@cmeri.res.in http://www.cmeri.res.in

Abstract: This paper focuses on the controller design procedure for any serial linked robot which articulates a typical snake like movement in surface level. Programmable smart DSP processor is used for high accuracy signal processing and smooth control of the actuator used in each joint of SLR. Different approaches like, frequency domain approach and graphical approach for controller design are discussed and the same are implemented in TMS320C6713 DSP processor to study the controller characteristics with their transient and impulse response. Results infer the difference between two transfer functions of DC motor controller designed in the above fashion with similar parameters.

Key-Words: - Snake-like motion, ACM, DSP processor, TMS320C6713

1 Introduction

The main challenge in the design of serial linked robot (SLR) deals with putting actuated joints in a tight volume where we minimize the length and cross sectional areas of the links between the joints. The main concept of this design is to stack two degrees-of-freedom (DoF) joints on top of each other, forming a serial linked robot. One of the most popular examples of SLR is snake like robot. Here the main challenge of design is divided into two basic parts: 1) Active Cord Mechanism (ACM) and 2) smart controller design to follow the trajectory with avoiding obstacles. In this paper, the main area of work is concentrated on designing a SLR and to achieve its exact ACM in simulation while implemented with DSP processor. The intermediate joints of the SLR are given sinusoidal input which results into a serpentine movement of the entire body.

Multi-segmented robots (e.g., SLR) have been studied for many years, particularly for their ability to deal with difficult environments, in which other types of robots often fail. One of first snake-like robot, named an active cord mechanism [1], has been constructed in 1972. Since then a variety of different snake robots have been designed [2], [3], [4], [5], and [6], some of which are currently used for the inspection of pipes [7], for example. A review of snake robots can be found in [8] and [9]. Most of these robots have been designed for locomotion on ground, and only a few working examples of swimming snake robots currently exist. The most interesting ones are the eel robot REEL II [10], the lamprey robot built at Northeastern University [11] and the spirochete-like HELIX-I [12]. Another work also carried away in [13], to build an amphibious snake-like robot that can both crawl and swim for outdoor robotics tasks, taking inspiration from snakes and elongate fishes such as lampreys, and to demonstrate the use of central pattern generators (CPGs) as a powerful method for online trajectory generation for crawling and swimming in a real robot. AmphiBot II, presented in [13], is the new version of AmphiBot I [14], [15], with comparison to its predecessor, features a significant number of improvements, like: A better mechanical design, more powerful motors, wireless communication capabilities, onboard CPG running on a microcontroller, therefore removing the need of running the controller on an external computer.

The next section of this article represents the mathematical modeling of ACM for any SLR, e.g. Serpentine movement. Section 3 illustrates the architecture of 6713 DSP processor with its advanced features to show its compatibility to our design unlike other processors which are compared with it in a tabulated format. In section 4 controller design procedure is described for SLR and finally, section 5 shows transient and impulse responses of the controller, designed and implemented in TMS320C6713 platform to process sinusoidal signal in real time.

2 Backbone Curve for Snake Like Locomotion:

To illustrate the dynamics of SLR we can refer to its most popular example i.e. serpentine robot for the ACM curve. In serpentine robot there is a sinusoidal movement along an axis which is the direction of propagation. Fig. 1-(a) and (b) shows a serpentine movement in two dimensional axes and its relevant ACM curve, respectively. The ACM executes its

winding movements by means of actuators positioned along its body. The ACM has an arbitrary configuration on a plane, and if it performs two-dimensional movements there, these can be expressed by the kinematic relationships expressed through equation 1 to 8.

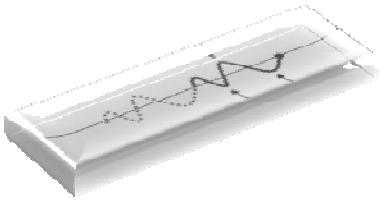

(a)

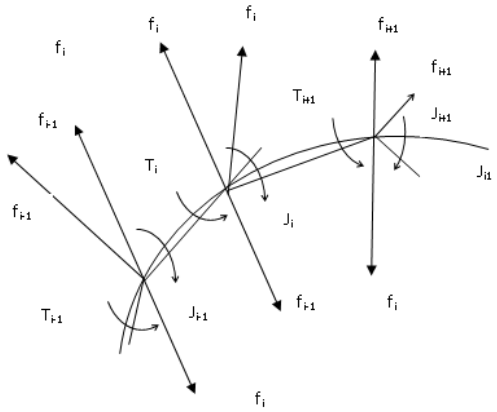

(b)

Fig 1: (a) Serpentine movement in 2-D, (b) ACM curve for Serpentine movement

When the actuator positioned at an arbitrary joint J_i gives rise to joint torque T_i, a force defined as,

$$f_i \triangleq \frac{T_i}{\delta s} \quad (1)$$

is produced at joint Ji and joints J_{i-1} , J_{i+1} or either side of it.

The tangential force density function ft(s), integrated over the whole body of the ACM (length L), is no longer than the propulsive force of the tangential force of the ACM. Consequently, if we call this the tangential force (propulsive force) and denote it Ft, we can express it as follows:

$$F_t=\int_0^L \frac{d\,T(s)}{ds}\,\rho(s)\,ds \quad (2)$$

Where, $\rho_i = \frac{\sigma_i}{\delta s}$, as δs is supposed to be infinitesimal.

When we consider the ACM's locomotive movement normal force is the force which resists external force and the total of the absolute values of the normal force over the body provides an indication of the efficiency of the ACM's locomotive movement. Accordingly, we will define this as normal force 'F_n', and express it as follows:

$$F_n=\int_0^L \left|\frac{d^2T(s)}{ds^2}\right| ds \quad (3)$$

Because of the limits to the power which the actuators positioned on the ACM's body can generate there are many cases when its posture and speed of movements are restricted. For this reason, in this section power can be formulated for a moving body with speed 'v' along body axis's'.

$$P_i = T_i \frac{d\Theta_i}{dt}$$

Or,

$$P(s)=T(s)\frac{d\,\rho(s)}{ds}v \quad (4)$$

Through equation (4) we express the torque distribution and curvature distribution by the continuous functions T(s), ρ(s) and the power density function is known as Pi/ δs.

During locomotion it is necessary that this value P(s) be below the maximum upper limit normally determined by the performance of the actuators.

On the basis that the hypothesis that the antagonistic muscle alternately repeat contracting and relaxing movements of uniform speed when the snake is gliding steadily, we can use the standard form of Fresnel's integrals and get the following expression for serpenoid curve:

$$x(s) = s\,J_0(\alpha) + \frac{4l}{\pi}\sum_{m=1}^{\infty} J_{2m}(\alpha)\left(\sin\ \frac{m\pi s}{l}\right) \quad (5)$$

$$y(s) = \frac{4l}{\pi}\sum_{m=1}^{\infty} \frac{(-1)^{m-1}\,J_{2m}(\alpha)}{2m-1}\left(\sin\ \frac{(2m-1)\pi s}{l}\right) \quad (6)$$

Where, Jn (α) is the Bessel function and is expressed as,

$$J_n(\alpha) = \left(\frac{\alpha}{2}\right)^n \sum_{m=0}^{\infty} \frac{(-1)^m}{m!\,\Gamma(n+m+1)}\left(\left(\frac{\alpha}{2}\right)^{2m}\right) \quad (7)$$

From previous work on the distribution of muscular force, σ was found to be a real number. Accordingly, the following new function is proposed in [16],

$$\text{Serp}\ (\sigma) = \left(\frac{2}{\pi}\right)^{\sigma}\int_0^{\frac{\pi}{2}} x^{\sigma-1}\sin x\ dx, \quad (8)$$

Given, $\sigma > 1$

3 Architecture of TMS320C6713 DSP Processor:

The TMS320C6713 DSP packs a powerful floating-point C67x DSP core along with enriched peripherals to achieve performance improvements over the industry's previous DSP performance leader, (Table-1),the TMS320C6701 DSP [17]. Chips in development couple this processing performance with new memory and peripheral systems designed to accelerate real-time throughput for higher system performance. The large internal memory and efficient on-chip cache architecture of the C6713 allows system designers to use slower, cheaper external-memory devices for data and program storage, while keeping the high-performance capabilities of the device. In addition, a cache helps programmers to achieve their performance goals faster, shortening code development and accelerating time to market. The enhanced direct memory access (EDMA) controller allows designers to optimize data organization in their systems. Capable of accessing any location in the C6713 memory map, the EDMA controller transfers data in the background of DSP core operation. The EDMA controller can handle multiple transfers simultaneously and can interleave bursts. The EDMA controller offers 16 independent channels, with a separate RAM space to hold additional transfer configurations. Each EDMA controller channel is synchronized by an event to allow minimal intervention by the DSP core. The on-chip memory is organized to allow design flexibility and ensure efficient memory usage. The C6713 has 264K bytes (KB) of on-chip memory

Unlike TMS320LF2407 DSP processor which has been used earlier in [18] for different application of robotics for its in-built ADCs and other features, TMS320C6713 has 32 bit data word, 225 MHz operating frequency , 32 bit of EMIF, 512 M byte addressable memory space and programmable clock generator. Table-1 distinguishes different DSP processors and Controllers in terms of their in-built features. Our selection of 6713 processor for its higher operating frequency, multitasking facility and larger memory space definitely makes the design of SLR smarter and more efficient in terms of accuracy and controller stability.

Table-1 has been referred to have a look on the technical specification of different DSP processors in TMS320XXXXX family followed by fig-2 which show the details of C6713 DSP architecture used in this controller.

Table: 1 Specification of Different DSP Processors

Part Number	Frequency (MHz)	CPU	On-Chip L1/SRAM	On-Chip L2/SRAM	EMIF	External Memory Type Supported	DMA	HPI	McBSP	McASP
TMS320C6713B-225	225	1 C67x	8 KB	64 KB Cache/192 KB SRAM	1 32-Bit	Async SRAM , SBSRAM , SDRAM	16 (EDMA)	1 16 Bit	2	2
TMS320C6712D-150	150	1 C67x	8 KB	64 KB	1 16-Bit	Async SRAM , SBSRAM , SDRAM	16-Ch EDMA		2	
TMS320C6711D-250	250	1 C67x	8 KB	64 KB	1 32-Bit	Async SRAM , SBSRAM , SDRAM	16-Ch EDMA	1 16 Bit	2	
TMS320C6711D-200	200	1 C67x	8 KB	64 KB	1 32-Bit	Async SRAM , SBSRAM , SDRAM	16-Ch EDMA	1 16 Bit	2	
TMS320C6701-150	150	1 C67x	8 KB	64KB	1 32-Bit	Async SRAM , SBSRAM , SDRAM	4-Ch DMA	1 16 Bit	2	

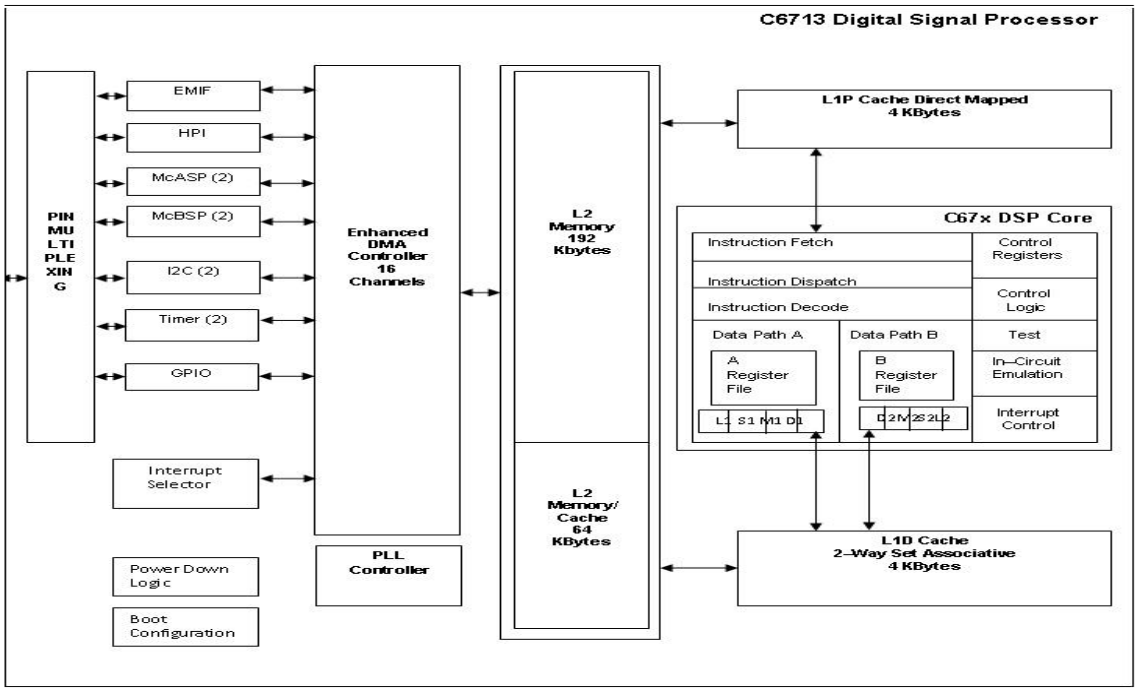

Fig 2: TMS320C6713 DSP architecture

4 Controller Design for Multi segmented Robot:

In an m-segment SLR, there are m-1 joints that are controlled to follow a perfect ACM curve. Each joint is supplied with a signal that needs to be controlled to achieve an overall serpentine movement. Here the main task is to design a DC motor controller for individual method, such as, Bode plot and Root Locus approach to compare the system transfer function $h_m(n)$ for the similar system in different method.Fig-3 shows the stages of designing a DSP based controller in CCS v 3.1 platform for the DC motor specified in Table-2 , used in developing the joints of the SLR. Fig-4 and 5 reflect the results of transient response and impulse response of the system obtained in TMS320C6713 platform.

The flow chart shown below in Fig-3 states the design procedure of DC motor controller for any SLR. The main advantage of SLR is that the total process of controller design for individual segment is repetitive in nature though the transfer function $h_m(n)$ of each controller has different impulse response shown in Fig-4 and 5. While we go for design of a controller we need to have some input regarding its gain margin (GM), phase margin (PM), maximum peak(M_p) ,rise time (t_r), settling time(t_s), etc. Hence we can calculate the damping ratio and undammed natural frequency to find the zeros and poles of the stable control system. The data(i). m file generated throughout the whole process contains the definition of each controller as i varies from 1 to m. Each *.m file generated in this process may consist n (here, =200) number of floating point values depending on the sampling rate(92 KSa/s) and operating frequency (225 MHz) of the DSP processor.

In this work 1.2 watt DC motor from MAXON Motor has been used which is smaller in size and suitable for our desired SLR. Table-2 shows detailed specification of this motor.

Table-2 Technical Specification of Maxon RE-max DC motor (model No.-203889), 1.2 watt

Parameter	Value
Armature Inductance*(La)*	0.223 mH
Armature Resistance *(Ra)*	11 ohm
Rotor Inertia*(Jm)*	0.306 gcm^2
Torque Constant*(Ki)*	5.08 mNm/A
No load Speed	11100 rpm
No load Current	10.4 mA
Speed/Torque Gradient	4050 rpm/mNm

Flow Chart:

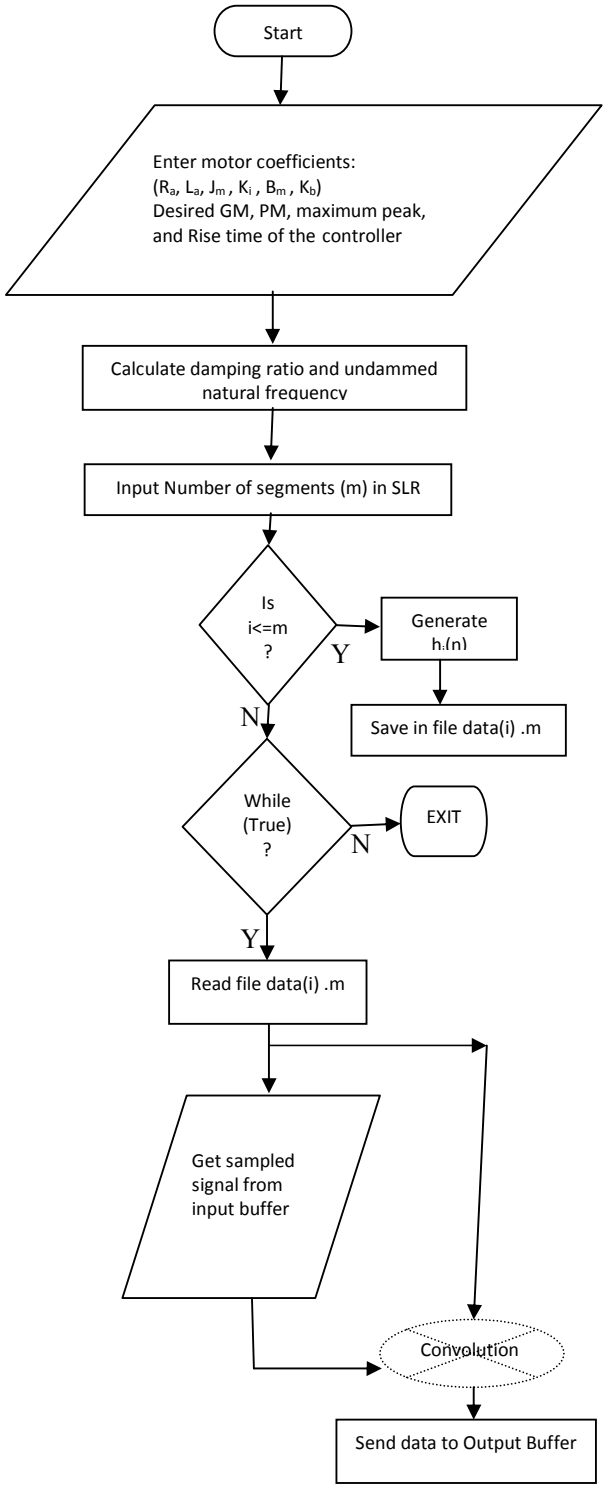

Fig-3 Flow chart of controller design procedure

5 Result Analysis:

A 4-segmented snake like robot is considered here for the realization of DC motor controller designed in Root-locus method and Bode Plot method, respectively. Specification of DC motor, cited at Table-2, has been used for controller design purpose. Simply for snake like locomotion in 2-D plane periodic sinusoidal wave has been targeted for generation by the entire snake body. As the whole body of SLR is segmented in four sections each section is responsible for $360^o/4= 90^o$ phase shift.

Each segment of serpentine robot is designed with TMS320C6713 DSP processor that is generally used for processing a sinusoidal signal to give a constant phase shift of 90^o so that the phase difference between the front end and rear end of the snake robot become zero. This DSP processor is also capable of processing communication signal upto 46 KHz (92 KSa/s) so that any wireless control from remote station is also possible with the help of some additional circuitry.

The graphical approach which is known as root locus approach has been followed to design DC motor controller and the gain, phase and pole-zero plot are shown in fig-4 followed by impulse response of individual segment controller and transient response of the entire system, respectively. Fig-5 demonstrates the bode plot approach which is also known as frequency response approach for controller design. A very good result has been achieved while processing similar sinusoidal signal. In root locus method a good amount of gain margin is achieved while in bode plot approach the phase of the system has been stabilized. Similarly, In root locus method the motor controller has become a overdamped system i.e. the output signal can never exceed the maximum voltage at the finest tuning while in bode plot method the rise time of 300ms and 25% of peak rise has been visualized in the transient response of the controller.

Following data are obtained as the output of the design procedure:

In root-locus method the designed controller has following specification:

Controller: Overdamped System
Gain Margin(GM): 46 dB
Phase Margin(PM):-180^o

In bode plot method the designed controller has following specification:

Controller: Uderdamped System
Rise time: 0.3 s
Maximum Peak: 25%
Gain Margin(GM):16.2 dB
Phase Margin(PM): 86.5^o

5.1 Graphical Method Approach or Root-Locus Approach

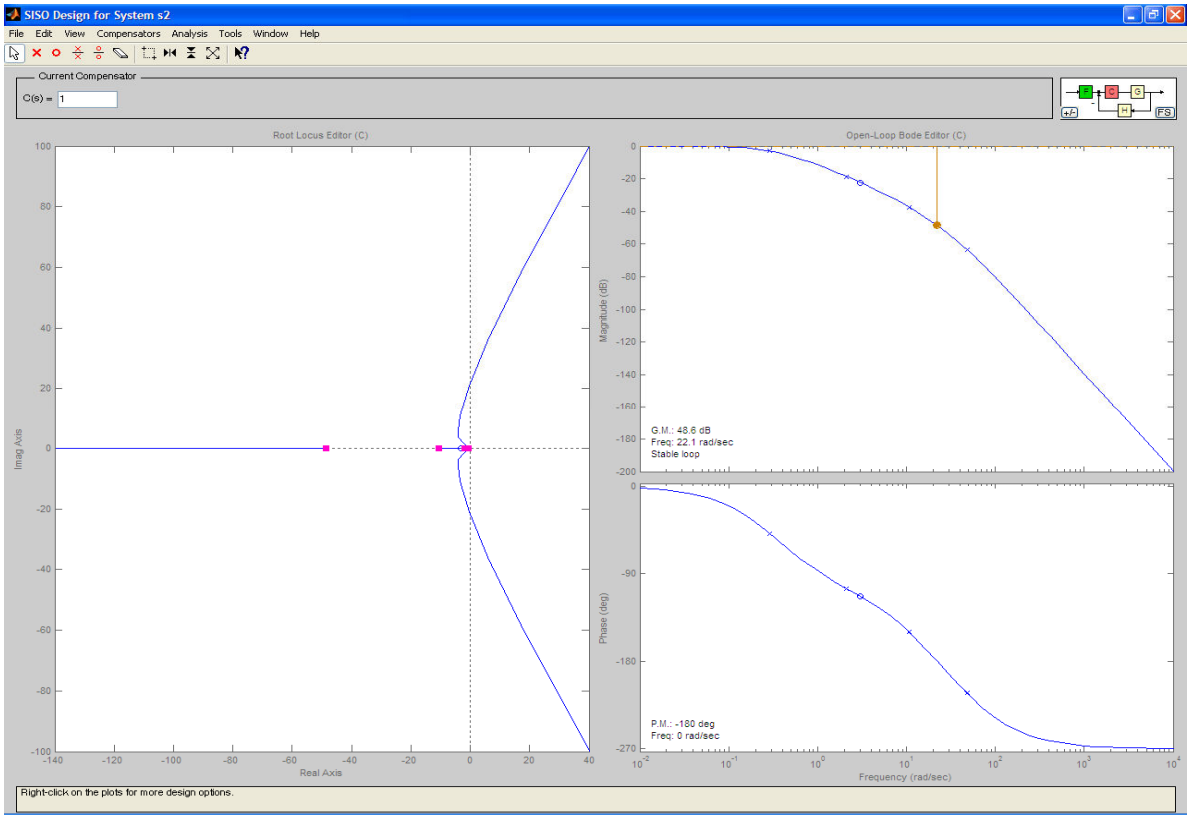

(a)

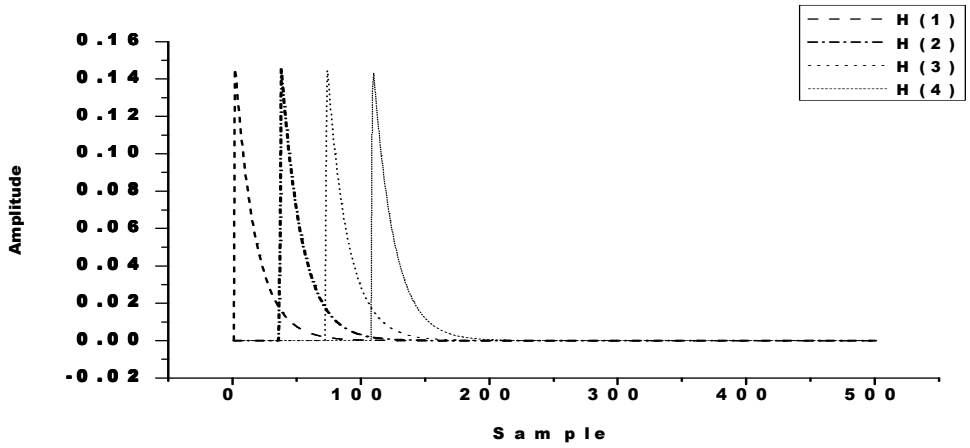

(b)

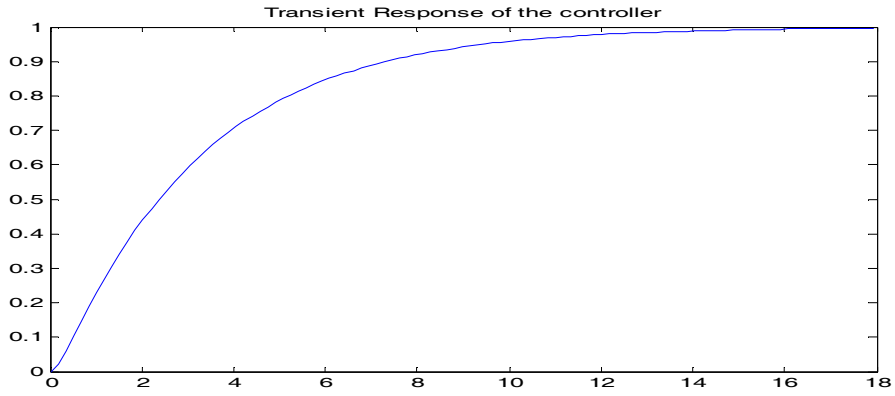

(c)

Fig.4 Result analysis of Graphical Method Approach or Root-Locus Approach (a) Stability analysis of Controlled system with Root locus and Bode plot, (b) Impulse Response of H(1),H(2),(H(3), H(4), and (c) Transient Response of DC motor Controller

5.2 Frequency Response Approach or Bode Plot Approach:

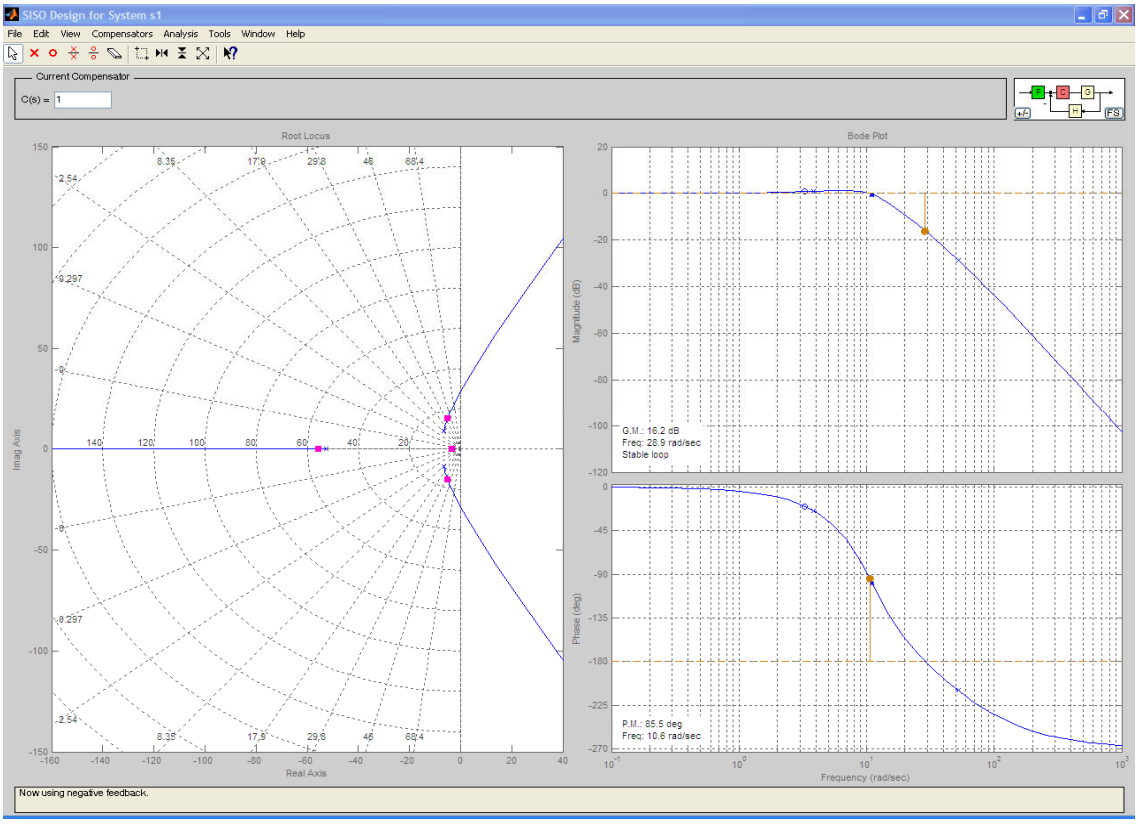

(a)

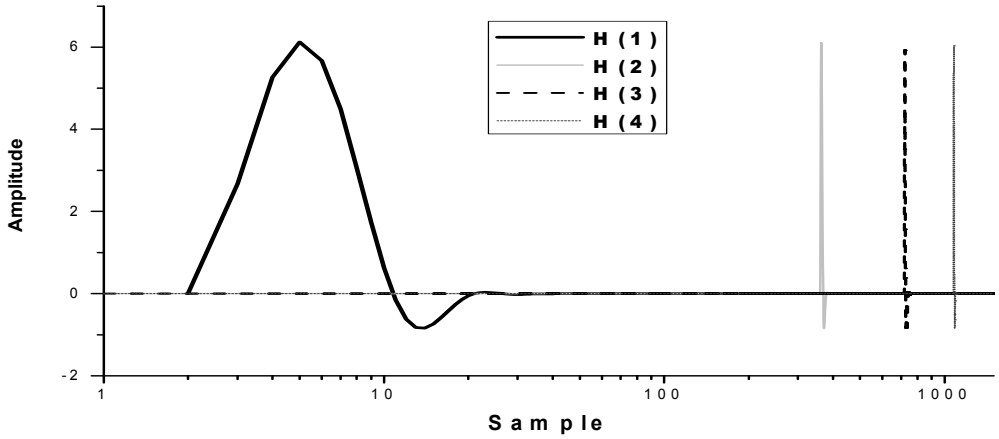

(b)

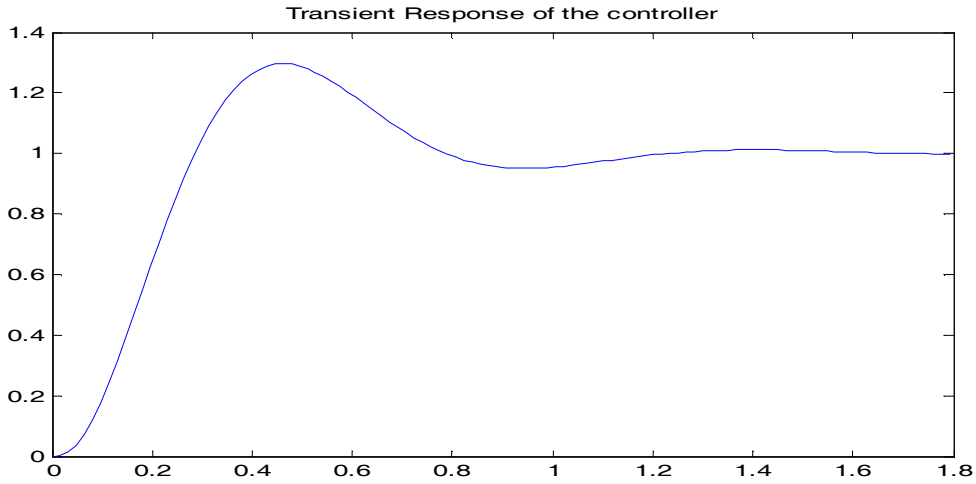

(c)

Fig.5 Result analysis of Frequency response approach or Bode plot approach (a) Stability analysis of Controlled system with Root locus and Bode plot, (b) Impulse Response of H(1),H(2),(H(3), H(4), and (c) Transient Response of DC motor Controller

6 Conclusion

Depending upon the application of serpentine robot the design procedure changes time to time. These above approaches have been materialized keeping in view the realization of basic biological behavior of serpentine robot. In advance cases like, obstacle avoidance with sensor data acquisition can also be implemented in this TMS320C6713 DSP platform. As the module is capable of processing communication signal remote control application may also be incorporated to enhance the rescue operation by serpentine robot. As the DSP processor uses PROM memory it is possible to program bidirectional movement of snake robot in certain circumstances.

References:

[1] Y. Umetani and S. Hirose, *Biomechanical study of activecord mechanism with tactile sensors*," in Proceedings of the6th international symposium on industrial robots, Nottingham, 1976, pp. c1-1{c1-10.

[2] G.S. Chirikjian and J.W. Burdick, *Design, implementation, and experiments with a thirty-degree-of-freedom `hyper-redundant' robot*," in ISRAM 1992, 1992.

[3] T. Lee, T. Ohm, and S. Hayati, *A highly redundant robot system for inspection*," in Proceedings of the conference on intellingent robotics in the ¯eld, factory, service, and space (CIRFFSS '94), Houston, Texas, 1994, pp. 142{149.

[4] K.L. Paap, M. Dehlwisch, and B. Klaassen, *GMD-snake:a semi-autonomous snake-like robot*," in Distributed Autonomous Robotic Systems 2. Springer-Verlag, 1996.

[5] B. Klaassen and K.L. Paap, *GMD-SNAKE2: A snake-likerobot driven by wheels and a method for motion control*," in ICRA 1999: Proceedings of 1999 IEEE International Conference on Robotics and Automation. 1999, pp. 3014{3019,IEEE.

[6] G.S.P. Miller, *Neurotechnology for biomimetic robots*, chapter Snake robots for search and rescue, Bradford/MIT Press,Cambridge London, 2002.

[7] H.R. Choi and S.M. Ryew, *Robotic system with active steering capability for internal inspection of urban gas,pipelines*," Mechatronics, vol. 12, pp. 713{736, 2002.

[8] K. Dowling, *Limbless Locomotion: Learning to Crawl with a Snake Robot*, Ph.D. thesis, Robotics Institute, Carnegie Mellon University, Pittsburgh, PA, December 1997.

[9] R. Worst, *Robotic snakes*," in Third German Workshop on Arti¯cal Life. 1998, pp. 113{126, Verlag Harri Deutsch.

[10] K.A. McIsaac and J.P. Ostrowski, *A geometric approach to anguilliform locomotion: Simulation and experiments with an underwater eel-robot*," in ICRA 1999: Proceedings of 1999 IEEE International Conference on Robotics and Automation. 1999, pp. 2843{2848, IEEE.

[11] C. Wilbur, W. Vorus, Y. Cao, and S.N. Currie, *Neurotechnology for biomimetic robots*, chapter A Lamprey-Based Undulatory Vehicle, Bradford/MIT Press, Cambridge London,2002.

[12] T. Takayama and S. Hirose, *Amphibious 3D active cordmechanism \HELIX" with helical swimming motion,*" inProceedings of the 2002 IEEE/RSJ International Confer-ence on Intelligent Robots and Systems. 2002, pp. 775{780,IEEE.

[13] Alessandro Crespi, Auke Jan Ijspeert "*AmphiBot II: An Amphibious Snake Robot that Crawls and Swimsusing a Central Pattern Generator*", Proceedings of the 9th International Conference on Climbing and Walking RobotsBrussels, Belgium - September 2006

[14] A. Crespi, A. Badertscher, A. Guignard, and A.J. Ijspeert,*AmphiBot I: An amphibious snake-like robot,*" Roboticsand Autonomous Systems, vol. 50, no. 4, pp. 163{175, 2005.

[15] A. Crespi, A. Badertscher, A. Guignard, and Ijspeert. A.J.,*Swimming and crawling with an amphibious snake robot*,"in Proceedings of the 2005 IEEE International Conference on Robotics and Automation (ICRA 2005), 2005, pp. 3035{3039.

[16] S. Hirose, "Biologically inspired Robots Snake like Locomotors and Manipulators", Oxford Science Publication, 1993.

[17] " *TMS320C6713B Floating Point Processor" SPRS294B* − OCTOBER 2005 − REVISED JUNE 2006, www.ti.com

[18] J. Xiao, Dulimarta. H, Zhenyu Yu, Ning Xi, "*DSP Solution for Wall-climber Microrobot Control using TMS320LF2407 Chip*", circuits and Systems, 2000; proceedings of the 43rd IEEE Midwest Symposium on vol. 3 , issue , 2000,page(s): 1348-1351,vol.3.